Published in final edited form as:

Mol Plant. 2022 February 07; 15(2): 354–362. doi:10.1016/j.molp.2021.11.001.

Lack of ethylene does not affect reproductive success and synergid cell death in *Arabidopsis*

Wenhao Li[1,5], **Qiyun Li**[1,5], **Mohan Lyu**[1,5], **Zhijuan Wang**[1], **Zihan Song**[1], **Shangwei Zhong**[1], **Hongya Gu**[1,2], **Juan Dong**[3], **Thomas Dresselhaus**[4], **Sheng Zhong**[1,*], **Li-Jia Qu**[1,2,*]

[1]State Key Laboratory for Protein and Plant Gene Research, Peking-Tsinghua Center for Life Sciences at College of Life Sciences, Peking University, Beijing 100871, People's Republic of China

[2]The National Plant Gene Research Center (Beijing), Beijing 100101, People's Republic of China

[3]The Waksman Institute of Microbiology, Rutgers the State University of New Jersey, Piscataway, NJ 08854, USA

[4]Cell Biology and Plant Biochemistry, University of Regensburg, 93053 Regensburg, Germany

[5]These authors contributed equally to this article.

Abstract

The signaling pathway of the gaseous hormone ethylene is involved in plant reproduction, growth, development, and stress responses. During reproduction, the two synergid cells of the angiosperm female gametophyte both undergo programmed cell death (PCD)/degeneration but in a different manner: PCD/degeneration of one synergid facilitates pollen tube rupture and thereby the release of sperm cells, while PCD/degeneration of the other synergid blocks supernumerary pollen tubes. Ethylene signaling was postulated to participate in some of the synergid cell functions, such as pollen tube attraction and the induction of PCD/degeneration. However, ethylene-mediated induction of synergid PCD/degeneration and the role of ethylene itself have not been firmly established. Here, we employed the CRISPR/Cas9 technology to knock out the five ethylene-biosynthesis 1-aminocyclopropane-1-carboxylic acid oxidase (ACO) genes and created *Arabidopsis* mutants free of ethylene production. The ethylene-free mutant plants showed normal triple responses when treated with ethylene rather than 1-aminocyclopropane-1-carboxylic acid, but had increased lateral root density and enlarged petal sizes, which are typical phenotypes of mutants defective in ethylene signaling. Using these ethylene-free plants, we further demonstrated that production of ethylene is not necessarily required to trigger PCD/degeneration of the two synergid cells, but certain components of ethylene signaling including transcription

*Correspondence: Sheng Zhong (shengshengzz@pku.edu.cn), Li-Jia Qu (qulj@pku.edu.cn).

AUTHOR CONTRIBUTIONS

L.-J.Q., and Sheng Zhong designed the study; and W.L., Sheng Zhong, Z.S. and Z.W. generated *ET-free* mutants; W.L., Q.L., and Sheng Zhong cultivated the hydroponic plants and analyzed the phenotypes; Q.L. and Sheng Zhong performed GC detection and analysis; M.L. and Shangwei Zhong performed the triple response and immunoblot experiments; L.-J.Q., Sheng Zhong, W.L., M.L., Shangwei Zhong, H.G., J.D., and T.D. interpreted the data and wrote the manuscript.

No competing interests declared.

SUPPLEMENTAL INFORMATION

Supplemental Information is available at *Molecular Plant Online*.

factors ETHYLENE-INSENSITIVE 3 (EIN3) and EIN3-LIKE 1 (EIL1) are necessary for the death of the persistent synergid cell.

Keywords

ethylene; ACC; PCD; synergid cells; triple response; *Arabidopsis*

INTRODUCTION

Ethylene is an important gaseous hormone in plants that is involved in the regulation of numerous cellular processes (Binder, 2020). The ethylene biosynthetic pathway consists of two enzymatic steps as described in Figure 1A. The activity of 1-aminocyclopropane-1-carboxylic acid (ACC) synthases (ACSs) is strongly modulated by environmental stresses and light, and is considered a rate-limiting step in ethylene biosynthesis (Dubois et al., 2018). ACC can also be conjugated to become malonyl-, γ-glutamyl-, or jasmonyl-ACC, so that the availability of ACC to be converted to ethylene is further fine-tuned. In addition, ACC is soluble and can be taken up by the amino acid transporter Lysine Histidine Transporter 1 (LHT1) and transported through the xylem to other parts of a plant where ACC is locally converted to ethylene (Dubois et al., 2018).

In *Arabidopsis thaliana*, ethylene is perceived by ER-localized receptors, including ETHYLENE RESPONSE SENSOR 1 (ERS1), ERS2, ETHYLENE RESPONSE 1 (ETR1), ETR2, and ETHYLENE-INSENSITIVE 4 (EIN4), which become inactive upon ethylene binding. In the absence of ethylene, these receptors activate a Raf-like Ser/Thr protein kinase, CTR1, to phosphorylate and inhibit EIN2, an ER-located membrane protein. In the presence of ethylene, inactivation of the receptors results in the release of CTR1-mediated inhibition on EIN2. As a consequence, EIN2 is cleaved and translocated to P-bodies where it promotes the stability of transcription factors EIN3 and EIN3-LIKE 1 (EIL1), leading to elevated expression of numerous downstream genes mediating ethylene responses (Binder, 2020; Zhang et al., 2020; Zhao et al., 2021). Ethylene has been reported to regulate a multitude of plant processes, including seed germination, seedling growth, organ senescence, fruit ripening, and pollen tube attraction (Zhang et al., 2018) as well as various responses to biotic and abiotic stresses (Dubois et al., 2018; Binder, 2020; Zhao et al., 2021). At the cellular level, ethylene alters cell elongation and chloroplast maturation (Liu et al., 2017), and has also been shown to induce programmed cell death (PCD) (Lam et al., 1999).

During angiosperm reproduction, PCD is closely associated with the function of the two synergid cells. Two immobile sperm cells are conveyed by a pollen tube toward the synergid cells (Zhang et al., 2017; Johnson et al., 2019). Directional growth of the pollen tube is directed by spatial cues from various female tissues prior to ultimately reaching the embryo sac for double fertilization (Higashiyama and Takeuchi, 2015; Qu et al., 2015). When the pollen tube enters the micropyle, one of the two synergid cells (i.e., receptive synergid) degenerates, allowing pollen tube reception, followed by pollen tube rupture and sperm cell release. During this process, the second synergid (i.e., persistent synergid) maintains its integrity. Once double fertilization is achieved, the persistent synergid degenerates in a

fertilization-dependent manner to prevent polytubey (the arrival of multiple pollen tubes). In the case of fertilization failure, the persistent synergid remains intact to attract secondary pollen tubes for another chance of fertilization (Hater et al., 2020). This mechanism has been referred to as fertilization recovery (Kasahara et al., 2012). Therefore, timely degeneration of both synergid cells is essential for reproductive success (Sandaklie-Nikolova et al., 2007; Vöz t al., 2013; Maruyama et al., 2015; Maruyama and Higashiyama, 2016).

Ethylene has been proposed to be involved in PCD/degeneration of the two synergid cells in *A. thaliana*. On the one hand, in the ethylene constitutive-response mutant *ctr1*, PCD/degeneration of the two synergid cells was observed in a fertilization-independent manner (Völz et al., 2013). Moreover, the two synergid cells underwent degeneration when the ethylene precursor ACC was injected into the large adjacent central cell (Völz et al., 2013). On the other hand, in the ethylene-insensitive mutants *ein3 eil1* and *ein2*, degeneration of the persistent synergid cell after fertilization was delayed, resulting in initiation of fertilization recovery and polytubey (Völz et al., 2013; Maruyama et al., 2015). These findings support the hypothesis that ethylene plays a key role in PCD/degeneration of the two synergid cells. This conclusion, however, was mainly based on the examination of embryo sacs artificially injected with ACC and the phenotypes of ethylene response component and constitutive ethylene-signaling mutants, but not on the effects of the hormone ethylene itself. Moreover, the major components of ethylene signaling have been reported to be simultaneously involved in other signaling pathways (Dubois et al., 2018; Binder, 2020; Zhao et al., 2021). Therefore, the phenotypes observed in ethylene response component mutants are not always necessarily attributable to ethylene; thus, there is a need for essential genetic evidence for final determination of the role of ethylene itself in synergid PCD/degeneration.

To address this question, we generated ACC oxidase (ACO) quintuple mutants in which all five *ACO* genes were inactivated and ethylene production thus abolished. Using these ethylene-free mutant plants, we examined PCD/degeneration of both receptive and persistent synergid cells under normal growth conditions. Our results demonstrate that in the absence of ACO activity, ACC itself cannot trigger ethylene signaling, and that ethylene production is not necessarily required for the death of the two synergid cells. However, as described below, other downstream components of the ethylene-signaling pathway do play a role in controlling the death of the persistent synergid cell.

RESULTS AND DISCUSSION

Generation of *ethylene-free* plants

The *Arabidopsis* genome contains five *ACO* genes. To clarify the roles of ethylene in synergid PCD/degeneration, we adopted a loss-of-function strategy by employing CRISPR/Cas9 technology to mutagenize all five *Arabidopsis AtACO* genes. We obtained two independent lines of homozygous quintuple mutants, named *Ethylene-free-1* (*ET-free-1*) and *−2* (Figure 1B). Sequencing data showed that both mutants harbor point mutations or long deletions in each of the five *AtACO* genes, leading to five truncated ACO proteins lacking the catalytic domain (Figure 1B and Supplemental Figure 1).

To create an ethylene-free environment for plant growth, we employed multiple approaches to minimize any possible influence of exogenous ethylene. First, *ET-free-1* and *−2* plants were hydroponically grown (Supplemental Figure 2) to eliminate ethylene emission from soil bacteria. Second, chambers used for growing *ET-free-1* and *−2* plants were distantly placed from those containing wild-type (WT) plants. Third, all growth chambers were placed in the basement of the laboratory building, which is at least 50 m away from the parking lot, to avoid any minute amount of ethylene from car exhaust, tobacco smoke, or other forms of combustion (Morgott, 2015). The open field around the laboratory building allows natural fresh air to constantly circulate at approximately 2900–500 standard cubic feet per minute. Fourth, glass beakers wrapped in thick dark paper (Supplemental Figure 2), rather than plastic boxes, were used for hydroponic growth of plants to eliminate any ethylene emitted from the plastics (Royer et al., 2018). Finally, an ethylene absorbent, potassium permanganate (10%, 0.3 kg) (Wang et al., 2018, 2021), was placed nearby *ET-free-1* and *−2* plants and replenished every week in each growth chamber to ensure an ethylene-free environment.

Confirmation of *ET-free* plants and an ethylene-free environment

Under these strictly controlled growth conditions, we found that overall plant growth and development of *ET-free-1* and *−2* plants were largely normal, with plants producing fully fertile siliques (Figure 1C and 1D; Supplemental Figure 3). By using gas chromatography (GC) analysis (ethylene detection limit ≥0.001 ppm) (Guzman and Ecker, 1990), we established that WT ovules and other plant tissues namely leaves, inflorescences, and seedlings produced ethylene, whereas ethylene could not be detected in any tested tissue of *ET-free* mutants (Figure 1E and Supplemental Figure 4). In conclusion, by mutating the five *AtACO* genes of *Arabidopsis* we generated plants incapable of generating ethylene.

To further characterize *ET-free* quintuple mutants grown in our restricted growth conditions, we compared the vegetative growth phenotypes of these biosynthesis mutants with those of ethylene-signaling mutants. Consistent with a previous report (Negi et al., 2008), 10-day-old seedlings of quintuple mutant plants exhibited a lateral root density comparable with that of the ethylene-insensitive mutant *ein2–5* (Li et al., 2015), which is significantly higher than that of WT plants (Figure 2A and 2B). Furthermore, flowers of 1.5-month-old quintuple mutants, like those of other ethylene-signaling mutants (Feng et al., 2015), had petal areas (*ET-free-2*, 2.4 ± 0.3, $n = 61$) comparable with those of the *ein2–5* mutant (2.4 ± 0.2, $n = 78$), but significantly larger than those of WT plants (2.1 ± 0.4, $n = 67$) (Figure 2C and 2D). Previous studies showed that treatment with external ethylene at concentrations lower than 0.01 ppm will not lead to observable phenotypes, such as reduced hypocotyl length (Hua and Meyerowitz, 1998). Here, pronounced vegetative growth defects highly resembling those of ethylene-signaling mutants were observed in *ET-free plants*. The results indicate that we were able to create an ethylene-free environment.

The triple response is not compromised in *ET-free* mutant plants

We next hypothesized that disabling ethylene biosynthesis should not affect ethylene responses. To test this hypothesis, we externally applied ethylene to dark-grown seedlings. We anticipated that the ethylene-biosynthesis mutants but not the signaling mutants would

show the so-called triple response, i.e., reduced hypocotyl elongation, hypocotyl swelling, and apical hook exaggeration upon ethylene treatment. Indeed, upon ethylene treatment, the ethylene-signaling mutants *ein3 eil1* and *ein2* failed to show the response, whereas the *ET-free* mutants behaved like WT seedlings (Figure 2E–2H and Supplemental Figure 5A–5D), indicating that the ethylene-signaling pathway was not affected in the *ET-free* mutants. However, when seedlings were treated with the ethylene precursor ACC, WT seedlings showed the triple response as previously reported (Hua and Meyerowitz, 1998), but neither *ein3 eil1*, *ein2*, nor the *ET-free* mutants showed the triple response (Figure 2I and 2J; Supplemental Figure 5E and 5F). Western blot analysis using an EIN3 antibody showed that endogenous EIN3 was induced by ethylene treatment and accumulated to a similar level in *ET-free* mutants as in WT plants, whereas a signal was not detected in *ein3 eil1* mutants, which were used as a negative control (Figure 2K). This indicates that, unlike in the *ein3 eil1* mutant, ethylene signaling is intact and complete in *ET-free* mutant plants. However, treatment with ACC induced accumulation of EIN3 in the WT, but not in the *ET-free* quintuple or *ein3 eil1* mutants (Figure 2L). This observation further demonstrates that in the absence of ACOs, ACC is not able to act as ethylene to induce the accumulation of EIN3. These findings indicate that ethylene itself, but not its precursor ACC, is the actual inducer of the triple response.

Neither ethylene nor ethylene signaling is necessarily needed for receptive synergid PCD/degeneration

Because *ET-free* quintuple mutant plants exhibited normal seed set and fertility (Figure 1D), we further tested the relevance of ethylene for PCD/degeneration of the receptive and persistent synergid cells. To better observe degeneration of the receptive synergid cell, we used the MYB98pro:H_2B-tdTOM marker, which specifically labels the nuclei of the two synergid cells. Intact nuclei appeared large and round and showed bright fluorescence, whereas either the absence of nuclei or defective, degenerated nuclei showed diffused, malformed, or condensed fluorescence (Leydon et al., 2015). We observed that the synergid cell status was comparable in unpollinated WT and *ET-free* mutants (Supplemental Figure 6), indicating that ethylene itself does not affect the synergid cell status in mature ovules. At 16 h after pollination (HAP), when almost all of the ovules were targeted by pollen tubes (Supplemental Figure 7A and 7B), intact synergid nuclei were almost no longer detectable in ovules of WT and *ET-free* mutants (Figure 3A and 3B). This showed that all synergid cells underwent PCD/degeneration. However, approximately 9% of *lre* mutant ovules (8.5 ± 1.0%, $n_r = 3$, $n_o = 351$), in which pollen tube recognition by the synergid cells is defective, still showed robust expression of the nuclear marker in both synergid cells (Figure 3A and 3B) (Capron et al., 2008; Leydon et al., 2015). These observations indicate that ethylene is not necessarily needed for PCD/degeneration of the receptive synergid cells in *Arabidopsis*.

Ethylene signaling but not necessarily ethylene itself is involved in persistent synergid PCD/degeneration

We next analyzed the synergid nuclear marker MYB98pro:H_2B-tdTOM in combination with a pollen tube cytoplasmic marker, LAT52pro:GFP, to investigate whether ethylene signaling affects the fate of the persistent synergid cell, which degenerates in a fertilization-dependent manner (Leydon et al., 2015). In the WT, at 16 HAP both synergid nuclei were no longer

detectable in most of the ovules (90.6% ± 1.5%, $n_r = 3$, $n_o = 307$), indicating that the majority of synergid nuclei were degenerated. A small percentage of ovules (9.3% ± 1.5%) still contained one intact synergid nucleus, presumably belonging to the persistent synergid (Figure 3C and 3F). Notably, the ethylene-signaling mutant *ein3 eil1* contained significantly higher ratios of ovules with one synergid nucleus at 16 HAP (23.6% ± 6.8%, $n_r = 3$, $n_o = 198$, $p < 0.01$) (Figure 3D and 3F), suggesting that ethylene-signaling components, i.e., EIN3 and EIL1, are required for efficient degeneration of the persistent synergid cell, as previously reported (Völz et al., 2013). Importantly, in selfed *ET-free-1 and ™2* mutants, about 92.7% ± 2.2% ($n_r = 3$, $n_o = 342$) and 91.6% ± 0.5% ($n_r = 3$, $n_o = 191$) of ovules lacked synergid nuclei at 16 HAP, respectively, comparable with WT ovules (Figure 3E and 3F). In conclusion, fertilization-induced PCD/degeneration of the persistent synergid cell is independent of ethylene itself but requires components of the ethylene-signaling pathway.

Degeneration of the persistent synergid cell facilitates prevention of supernumerary pollen tube arrival at fertilized ovules, whereas prolonged integrity of persistent synergid cells increases the rate of polytubey and the release of extra sperm cells. Therefore, we further examined the occurrence of polytubey in different genetic backgrounds. At 48 HAP, about 52.7% ± 10.6% ($n_s = 14$) of *ein3 eil1* ovules were targeted by more than one pollen tube, whereas the number was 13.6% ± 6.0% ($n_s = 12$, $P < 0.01$ versus *ein3 eil1*) for WT ovules (Figure 3G and 3H). In *ET-free* mutants, the polytubey ratio was 10.8% ± 3.6% for *ET-free-1* ($n_s = 18$, $P > 0.05$ versus WT, $P < 0.01$ versus *ein3 eil1*) and 11.5% ± 5.2% for *ET-free-2* ($n_s = 10$, $P > 0.05$ versus WT, $P < 0.01$ versus *ein3 eil1*) (Figure 3G and 3H). This further confirms that PCD/degeneration of persistent synergid cells is not discernibly affected by the lack of ethylene.

It was previously shown that manual injection of ACC into the female gametophyte triggers synergid cell death (Völz et al., 2013). We suggest that this is likely a result of overproduction of ethylene, similar to that for the constitutive ethylene-signaling mutant *ctr1* (Kieber et al., 1993), through synergid cell-expressed ACO5, which originally converts ACC to ethylene in WT plants (Supplemental Figure 8). ACC has recently been proposed to mediate an independent signaling pathway controlling pollen tube attraction, since ACS octuplet mutant plants exhibited defects in pollen tube attraction and fertility (Mou et al., 2020). Our observation that *ET-free* mutant plants exhibit normal fertility confirms that the fertility defects observed in the *acs* octuplet mutants were not due to the loss of ethylene production but were instead caused by the loss of ACC. However, how ACC implements its ethylene-signaling-independent function, for example to trigger calcium and/or other signaling pathways in plant cells (Mou et al., 2020), is still unclear. The *ET-free* mutants will provide a useful resource to distinguish the independent functions of ACC and ethylene in plant development and stress responses.

Based on the thorough investigation of *ET-free* mutants, we conclude that the gaseous hormone ethylene is not necessarily needed for reproductive success in unstressed plants, which is different from a previous conclusion (Zhang et al., 2018). This is probably due to the fact that ethylene is mainly involved in responses to biotic/abiotic stresses as well as in specific developmental processes (such as senescence and fruit ripening) that are not essential for fertility under favorable conditions, nor for PCD/degeneration of both

receptive and persistent synergid cells in *Arabidopsis*. However, certain components of ethylene signaling, including the EIN3 and EIL1 transcription factors, but not ethylene per se, are involved in the degeneration of the persistent synergid cell (Völz et al., 2013; Maruyama et al., 2015; Maruyama and Higashiyama, 2016). Our findings also support the idea that a possible ethylene independent signaling pathway with shared components of the ethylene-signaling cascade is involved in control of persistent synergid cell death. This ethylene-independent signaling pathway may control the death of the persistent synergid cell individually or collectively with the ethylene-signaling pathway. It is also clear that the defect in ethylene biosynthesis does not affect ethylene signaling, and that, without conversion into ethylene, ACC treatment does not trigger ethylene signaling and thus a triple response. Thus ACC possibly mediates another ethylene-independent signaling pathway using different downstream components. Currently, a number of environmental cues, such as light, salt, glucose, and phytohormones including auxin, jasmonic acid (JA), gibberellic acid (GA), cytokinins, and abscisic acid are known to interact with multiple components in the ethylene-signaling pathway (Dubois et al., 2018; Binder, 2020; Zhao et al., 2021). For example, EIN2 is a reported component in glucose-target-of-rapamycin signaling, which mediates growth in *Arabidopsis* (Fu et al., 2021), whereas the stability of the EIN3 protein is simultaneously regulated by light (Shi et al., 2016) and other phytohormones (such as JA and GA) as well as abiotic stresses (such as cold and salt) (Hao et al., 2017). Moreover, high levels of EIN3 were shown to disrupt pollen tube attraction (Zhang et al., 2018). Therefore, it will be exciting to elucidate how the activity of these shared components, in particular the EIN3 and EIL1 transcription factors, is regulated to coordinate fertilization-dependent degeneration of synergid cells.

MATERIALS AND METHODS

Plant material and growth conditions

A. thaliana ecotype Columbia-0 (Col-0) was used as the WT. All transgenic plants in this study were in the Col-0 background. *ET-free* mutants were obtained using CRISPR/Cas9 technology. The mutant *ein2–5* was previously reported in Li et al. (2015). For hydroponic growth, seeds were first surface sterilized, sown on half-strength Murashige–Skoog (1/2MS) medium, and cold-treated at 4°C for 2 days. Treated seeds were transferred to a growth chamber (Percival, AR-36L3) under long-day conditions (16 h light/8 h dark) at 22°C ± 2°C for 10 days. Seedlings were transferred onto aluminum foil in a hydroponic box with Hoagland nutrient solution (Hopebio HB8870–1) and continuously grown under long-day conditions as described above.

Plasmid constructs

The egg cell-targeting CRISPR/Cas9 system (Zhong et al., 2019) was used to obtain *AtACO1–5* quintuple mutants. Five pairs of single guide RNAs (sgRNAs) named *sgRNA1–10* were designed to target *AtACO1–5*. The dual spacer AtACO1_sgRNA1_U6_26t-U6_29p-AtACO1_sgRNA2 was amplified using primers including the sgRNA sequence from pCBCDT1T2 and then cloned into pENTR-AtU6–26 to produce pENTR-AtU6–26-sp1. pENTR-AtU6–26-sp2 to -sp5 were produced similarly. Restriction enzymes *Xba*I/*Hin*dIII and *Spe*I/*Hin*dIII were used to digest pENTR-AtU6–26-sp1 and pENTR-AtU6–26-

sp2, respectively. Fragments were ligated to produce pENTR-AtU6–26-sp1-sp2. Similarly, pENTRAtU6–26-sp4 and pENTR-AtU6–26-sp5 were digested and ligated to generate pENTR-AtU6–26-sp4-sp5. Next, pENTR-AtU6–26-sp3 was integrated into pENTR-AtU6–26-sp1-sp2 to produce pENTR-AtU6–26-sp1-sp2-sp3. pENTR-AtU6–26-sp1-sp2-sp3 and pENTR-AtU6–26-sp4-sp5 were treated similarly to generate pENTR-AtU6–26-sp1-sp2-sp3-sp4-sp5. Finally, pENTR-AtU6–26-sp1-sp2-sp3-sp4-sp5 was cloned into the destination vector pHEE401E.

For observation of the expression of *ACO5*, promoters and fragments containing the promoters and gene body regions without the stop codons of *AtACO1–5* were amplified and cloned into pENTR/D-TOPO through a TOPO reaction or pDONR221 through a BP reactions (Invitrogen). They were then cloned into the destination vectors pB7GUSWG0 (modified from pB7WGR2, VIB-Ghent University) and pK7FWG0 by performing LR reactions (Invitrogen) to generate the AtACO5pro:GUS and AtACO5pro:A-tACO5-GFP constructs, respectively. All primers used are listed in Supplemental Table 1.

To observe degeneration of synergid cells, we amplified the *MYB98* promoter and H_2B-tdTOM and cloned them into pDONR P4-P1r and pDONR221, respectively, through BP reactions (Invitrogen). Amplified fragments were then cloned into the destination vector pBm42GW3 (VIB-Ghent University) by performing LR reactions (Invitrogen) to generate the MYB98pro:H_2B-tdTOM construct. All primers used are listed in Supplemental Table 1.

Genotyping

Primers near the locus of the spacers on *AtACO1–5* and near the mutation sites of *EIN3* and *EIL1* (Zhong et al., 2009) were designed to identify the *ET-free* and *ein3 eil1* mutants. Genomic DNA from mutant plants was extracted from leaves. PCR and sequencing were used to identify deletions and point mutations, respectively, using the primers shown in Supplemental Table 1. Cas9-free mutants were identified by PCR with primers listed in Supplemental Table 1.

Ethylene detection

Stamens of floral stage 12 flowers were emasculated and ovary walls removed as previously reported (Johnson and Kost, 2010) at 36 h after emasculation. Next, three emasculated pistils (without ovary wall) were each placed in a 10-ml glass cuvette filled with 5 ml of 1/2MS medium and sealed with a rubber plug and parafilm. Ethylene detection (Guzman and Ecker, 1990) was performed after 2 days using a GC-2014 instrument (Shimadzu, Japan) via which at least 0.001 ppm ethylene is accurately detectable. Other plant tissues, namely 10-day-old seedlings and leaves and inflorescences taken from 35-day-old plants, were also analyzed using the same method. Three seedlings, three leaves, and one inflorescence were used for measurements. All experiments were repeated at least three times.

Phenotypic analysis

Seeds were sterilized with 70% ethanol solution for 15 min and washed six times with sterilized water. Seeds were sown on 1/2MS medium and cold-treated at 4°C for 2 days. Plates with treated seeds were placed vertically and transferred to a growth chamber

(Percival, AR-36L3) under long-day conditions (16 h light/8 h dark) at 22°C ± 2°C for 10 days. *ET-free-1* and *−2* seedlings were grown in isolated growth chambers. Seedlings were photographed, and lateral root numbers on the primary roots were counted using an M205FA microscope (Leica, Germany). The length of primary roots was measured by ImageJ (https://imagej/nih/gov/ij/), and the numbers of lateral roots were normalized to the primary root length (Susmita et al., 2020). About 20 seedlings were counted for each genotype.

Petals from flowers at stage 14–15 (maximum expansion) of hydroponic-grown plants were carefully dissected and placed on 1/2MS plates. Petals were photographed using an M205FA microscope (Leica), and the area of petals was measured by ImageJ (https://imagej/nih/gov/ij/). At least 60 petals were measured for each genotype.

Triple response measurement

Seeds were sterilized with 75% ethanol solution containing 0.05% Triton X-100 for 10 min and washed four times with sterilized water. Seeds were placed on 1/2MS medium and kept at 4°C for 3 days for stratification and irradiated under light for 8 h to stimulate germination. ACC (10 μM) was added to MS medium-containing plates for ACC treatment. For ethylene treatment, ethylene gas was injected into a glass beaker wrapped with plastic film with a final concentration of 10 ppm. To observe seedlings' phenotypes in darkness, we grew seeds in the dark at 22°C for 4 days. For each set of experiments, images of individual seedlings were obtained using a Leica M205FA Microsystem. Hypocotyl length was measured by ImageJ software (https://imagej/nih/gov/ij/).

Immunoblot assay

Seedlings were harvested, placed in a tube, and ground into powder with liquid nitrogen under green light. Proteins were extracted from the powder with extraction buffer (50 mM Tris–HCl [pH7.5], 1 mM $MgCl_2$, 150 mM NaCl, 0.1% Tween 20, 1× Roche complete EDTA-free protease inhibitor cocktail, and 1 mM phenylmethylsulfonyl fluoride). Extraction buffer with proteins was boiled and centrifuged before separation on a 10% SDS-polyacrylamide gel. An EIN3 antibody was used to detect EIN3 protein levels (Wu et al., 2020). Anti-actin (JF53–10, 1:10 000 dilution; Invitrogen) was used as a control for immunoblot analyses.

Aniline blue staining

For aniline blue staining, stamens of floral stage 12 flowers were emasculated. All pollinations were conducted at 36 h after emasculation. For visualization of pollen tube behavior, pollinated pistils were excised and fixed in FAA solution (acetic acid/EtOH [1:3] solution) for 2–4 h, followed by rehydration through a graded ethanol series of 70%, 50%, 30%, and ddH_2O. Samples were further softened with 8 M NaOH overnight at room temperature and then washed three times with water. Pollen tubes were stained with 0.1% decolorized aniline blue (pH 9–11, in 108 mM K_3PO_4) overnight. Stained samples were observed under a BX51 fluorescence microscope (Olympus) equipped with a UV filter set.

Microscopy

For ACO5pro:GUS observation, images were observed and collected using a BX51 fluorescence microscope (Olympus). To observe the localization of ACO5 using ACO5pro:ACO5-GFP with MYB98pro:H_2B-tdTOM reporter and the degeneration of the synergid cells using the MYB98pro:H_2B-tdTOM reporter, fluorescence images were observed and collected using an A1R confocal laser scanning microscope (Nikon). A 40× water objective lens was used for observation of the marker label under 488 nm or 561 nm.

ACCESSION NUMBERS

Data and materials generated in this study are available without restriction upon reasonable request from the corresponding author. Source data for all figures are provided with the paper.

Supplementary Material

Refer to Web version on PubMed Central for supplementary material.

ACKNOWLEDGMENTS

We thank Jianguo Yang (Peking University, China) for technical help in ethylene detection by GC. We are grateful to Qiguang Wen (Institute of Plant Physiology and Ecology, CAS, China) for discussions on ethylene signaling.

FUNDING

This work was supported by the National Key R&D Program of China (grant no. 2018YFE0204700) and National Natural Science Foundation of China (grant no. 31991202, 31830004, 31620103903, and 31621001 to L.-J.Q., and 32070854 to Sheng Zhong). The Qu laboratory is supported by the Peking-Tsinghua Joint Center for Life Sciences, and work on fertilization and early embryogenesis in the Dresselhaus lab is supported by the German Research Foundation DFG via Collaborative Research Center SFB960.

REFERENCES

Binder BM (2020). Ethylene signaling in plants. J. Biol. Chem. 295:7710–7725. [PubMed: 32332098]

Capron A, Gourgues M, Neiva LS, Faure JE, Berger F, Pagnussat G, Krishnan A, Alvarez-Mejia C, Vielle-Calzada JP, Lee YR, et al. (2008). Maternal control of male-gamete delivery in *Arabidopsis* involves a putative GPI-anchored protein encoded by the LORELEI gene. Plant Cell 20:3038–3049. [PubMed: 19028964]

Dubois M, Van den Broeck L, and Inze D (2018). The pivotal role of ethylene in plant growth. Trends Plant Sci. 23:311–323. [PubMed: 29428350]

Feng G, Liu G, and Xiao J (2015). The *Arabidopsis* EIN2 restricts organ growth by retarding cell expansion. Plant Signal. Behav. 10:e1017169. [PubMed: 26039475]

Fu L, Liu Y, Qin G, Wu P, Zi H, Xu Z, Zhao X, Wang Y, Li Y, Yang S, et al. (2021). The TOR—EIN2 axis mediates nuclear signalling to modulate plant growth. Nature 591:288–292. [PubMed: 33658715]

Guzman P, and Ecker JR (1990). Exploiting the triple response of *Arabidopsis* to identify ethylene-related mutants. Plant Cell 2:513–523. [PubMed: 2152173]

Hao D, Sun X, Ma B, Zhang J-S, and Guo H (2017). Ethylene. In in Hormone Metabolism and Signaling in Plants, Li J, Li C, and Smith SM, eds. (USA: Elsevier), pp. 203–241.

Hater F, Nakel T, and Gross-Hardt R (2020). Reproductive multitasking: the female gametophyte. Annu. Rev. Plant Biol. 71:517–546. [PubMed: 32442389]

Higashiyama T, and Takeuchi H (2015). The mechanism and key molecules involved in pollen tube guidance. Annu. Rev. Plant Biol. 66:393–413. [PubMed: 25621518]

Hua J, and Meyerowitz EM (1998). Ethylene responses are negatively regulated by a receptor gene family in *Arabidopsis thaliana*. Cell 94:261–271. [PubMed: 9695954]

Johnson MA, and Kost B (2010). Pollen tube development. In Plant Developmental BNiology: Methods and Protocols, Henning L and Köhler C, eds., *655*.. Methods in Molecular Biology (Methods and Protocols) (Totowa, NJ: Humana Press), pp. 155–176.

Johnson MA, Harper JF, and Palanivelu R (2019). A fruitful journey: pollen tube navigation from germination to fertilization. Annu. Rev. Plant Biol. 70:809–837. [PubMed: 30822112]

Kasahara RD, Maruyama D, Hamamura Y, Sakakibara T, Twell D, and Higashiyama T (2012). Fertilization recovery after defective sperm cell release in *Arabidopsis*. Curr. Biol. 22:1084–1089. [PubMed: 22608509]

Kieber JJ, Rothenberg M, Roman G, Feldmann KA, and Ecker JR (1993). CTR1, a negative regulator of the ethylene response pathway in *Arabidopsis*, encodes a member of the raf family of protein kinases. Cell 72:427–441. [PubMed: 8431946]

Lam E, Pontier D, and del Pozo O (1999). Die and let live— programmed cell death in plants. Curr. Opin. Plant Biol. 2:502–507. [PubMed: 10607660]

Leydon AR, Tsukamoto T, Dunatunga D, Qin Y, Johnson MA, and Palanivelu R (2015). Pollen tube discharge completes the process of synergid degeneration that is initiated by pollen tube-synergid interaction in *Arabidopsis*. Plant Physiol. 169:485–496. [PubMed: 26229050]

Li W, Ma M, Feng Y, Li H, Wang Y, Ma Y, Li M, An F, and Guo H (2015). EIN2-Directed translational regulation of ethylene signaling in *Arabidopsis*. Cell 163:670–683. [PubMed: 26496607]

Liu X, Liu R, Li Y, Shen X, Zhong S, and Shi H (2017). EIN3 and PIF3 form an interdependent module that represses chloroplast development in buried seedlings. Plant Cell 29:3051–3067. [PubMed: 29114016]

Maruyama D, and Higashiyama T (2016). The end of temptation: the elimination of persistent synergid cell identity. Curr. Opin. Plant Biol. 34:122–126. [PubMed: 27837692]

Maruyama D, Volz R, Takeuchi H, Mori T, Igawa T, Kurihara D, Kawashima T, Ueda M, Ito M, Umeda M, et al. (2015). Rapid elimination of the persistent synergid through a cell fusion mechanism. Cell 161:907–918. [PubMed: 25913191]

Morgott DA (2015). Anthropogenic and biogenic sources of ethylene and the potential for human exposure: a literature review. Chem. Biol. Interact. 241:10–22. [PubMed: 26296759]

Mou W, Kao YT, Michard E, Simon AA, Li D, Wudick MM, Lizzio MA, Feijo JA, and Chang C (2020). Ethylene-independent signaling by the ethylene precursor ACC in *Arabidopsis* ovular pollen tube attraction. Nat. Commun. 11:4082. [PubMed: 32796832]

Negi S, Ivanchenko MG, and Muday GK (2008). Ethylene regulates lateral root formation and auxin transport in *Arabidopsis thaliana*. Plant J. 55:175–187. [PubMed: 18363780]

Qu L-J, Li L, Lan Z, and Dresselhaus T (2015). Peptide signalling during the pollen tube journey and double fertilization. J. Exp. Bot. 66:5139–5150. [PubMed: 26068467]

Royer SJ, Ferron S, Wilson ST, and Karl DM (2018). Production of methane and ethylene from plastic in the environment. PLoS One 13:e0200574. [PubMed: 30067755]

Sandaklie-Nikolova L, Palanivelu R, King EJ, Copenhaver GP, and Drews GN (2007). Synergid cell death in *Arabidopsis* is triggered following direct interaction with the pollen tube. Plant Physiol. 144:1753–1762. [PubMed: 17545508]

Shi H, Shen X, Liu R, Xue C, Wei N, Deng XW, and Zhong S (2016). The red light receptor phytochrome B directly enhances substrate-E3 ligase interactions to attenuate ethylene responses. Dev. Cell 39:597–610. [PubMed: 27889482]

Susmita MM, Eshan S, Brinderjit S, and Jitendra PK (2020). Drought-induced protein (Di19–3) plays a role in auxin signaling by interacting with IAA14 in *Arabidopsis*. Plant Direct 4:e00234. [PubMed: 32582877]

Völz R, Heydlauff J, Ripper D, von Lyncker L, and Gross-Hardt R (2013). Ethylene signaling is required for synergid degeneration and the establishment of a pollen tube block. Dev. Cell 25:310–316. [PubMed: 23673332]

Wang B, Wang Y, Li W, Zhou J, Chang H, and Golding JB (2021). Effect of 1-MCP and ethylene absorbent on the development of lenticel disorder of 'Xinli No.7' pear and possible mechanisms. J. Sci. Food Agric. 101:2525–2533. [PubMed: 33063328]

Wang S, Zhou Q, Zhou X, Wei B, and Ji S (2018). The effect of ethylene absorbent treatment on the softening of blueberry fruit. Food Chem. 246:286–294. [PubMed: 29291851]

Wu QQ, Kuang KY, Lyu MH, Zhao Y, Li Y, Li J, Pan Y, Shi H, and Zhong SW (2020). Allosteric deactivation of PIFs and EIN3 by microproteins in light control of plant development. Proc. Natl. Acad. Sci. U S A 117:18858–18868. [PubMed: 32694206]

Zhang C, Teng XD, Zheng QQ, Zhao YY, Lu JY, Wang Y, Guo H, and Yang ZN (2018). Ethylene signaling is critical for synergid cell functional specification and pollen tube attraction. Plant J. 96:176–187. [PubMed: 30003612]

Zhang J, Chen Y, Lu J, Zhang Y, and Wen CK (2020). Uncertainty of EIN2Ser645/Ser924 inactivation by CTR1-mediated phosphorylation reveals the complexity of ethylene signaling. Plant Commun. 1:100046. [PubMed: 33367241]

Zhang J, Huang Q, Zhong S, Bleckmann A, Huang J, Guo X, Lin Q, Gu H, Dong J, Dresselhaus T, et al. (2017). Sperm cells are passive cargo of the pollen tube in plant fertilization. Nat. Plants 3:17079. [PubMed: 28585562]

Zhao H, Yin CC, Ma B, Chen SY, and Zhang JS (2021). Ethylene signaling in rice and *Arabidopsis*: new regulators and mechanisms. J. Integr. Plant Biol. 63:102–125. [PubMed: 33095478]

Zhong S, Zhao M, Shi T, Shi H, An F, Zhao Q, and Guo H (2009). EIN3/EIL1 cooperate with PIF1 to prevent photo-oxidation and to promote greening of *Arabidopsis* seedlings. Proc. Natl. Acad. Sci. U S A 106:21431–21436. [PubMed: 19948955]

Zhong S, Liu M, Wang Z, Huang Q, Hou S, Xu YC, Ge Z, Song Z, Huang J, Qiu X, et al. (2019). Cysteine-rich peptides promote interspecific genetic isolation in *Arabidopsis*. Science 364:eaau9564.

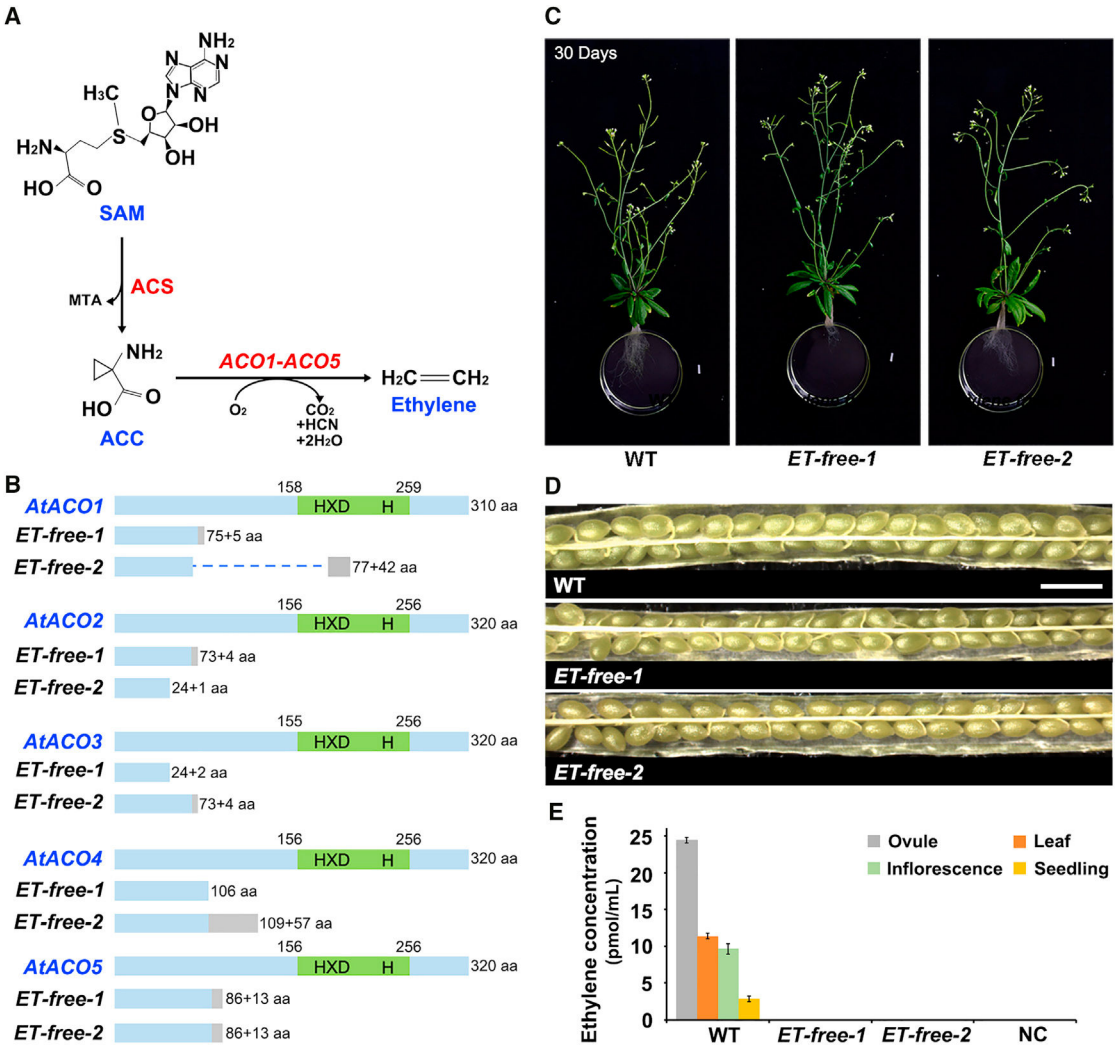

Figure 1. *ET-free* mutants show normal fertility during silique development.

(A) Ethylene biosynthesis from *S*-adenosyl methionine (SAM) via the intermediate 1-aminocyclopropane-1-carboxylic acid (ACC) is a two-step process catalyzed by ACC synthases (ACSs) and ACC oxidases (ACOs).

(B) Schematic diagram of all *Arabidopsis* ACOs containing an HXD motif and a catalytic site (H domain, both in green). Structures of CRISPR/Cas9-edited ACOs in *ET-free-1* and *ET-free-2* mutants are shown below full-length protein sequences. The numbers define the position of the conserved domains. aa, amino acid. Gray boxes indicate missense sequences due to frameshift mutations. Imaginary line indicates deleted protein sequence.

(C) Thirty-day-old hydroponic-grown wild-type (WT) and *ET-free* mutant plants. Scale bars, 0.8 cm.

(D) Siliques of WT and *ET-free* mutants. Scale bars, 1 mm.

(E) Analysis of ethylene concentration in different tissues of WT, *ET-free* mutant, and negative control (NC) plants by GC. Data are mean values ± SD.

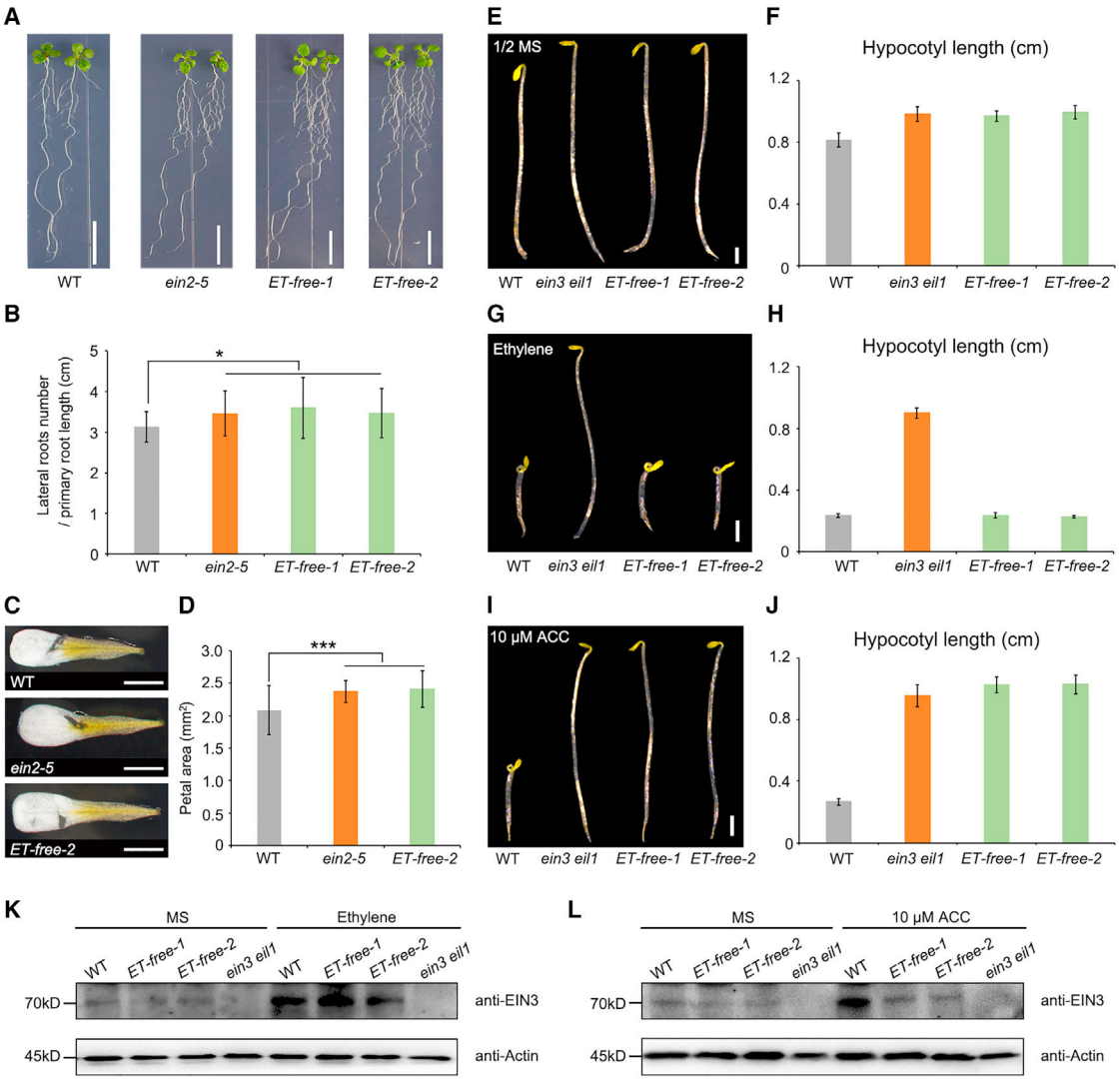

Figure 2. *ET-free* mutants shows that ethylene but not its precursor ACC is responsible for the triple response.

(A and B) Representative images and statistical analysis of lateral root density (number of lateral roots/primary root length [cm]) in WT ($n = 22$), *ein2–5* ($n = 22$), and *ET-free* mutants (*ET-free-1*, $n = 20$; *ET-free-2*, $n = 20$).

(C and D) Representative images and statistical analysis of petal area in WT ($n = 67$), *ein2–5* ($n = 78$), and *ET-free* mutants ($n = 61$). Scale bars, 1 cm.

(E–J) Triple response of WT, *ein3 eil1*, and *ET-free* mutants. **(E and F)** Seedlings grown on 1/2MS medium, and statistical analysis of hypocotyl length. **(G and H)** Seedlings grown on 1/2MS medium with 10 ppm ethylene treatment in darkness for 4 days, and statistical analysis of hypocotyl length. **(I and J)** Seedlings grown on 1/2MS medium in darkness for 4 days treated with 10 μM ACC, and corresponding statistical analysis of hypocotyl length. Scale bars, 1 mm.

(K and L) Immunoblots showing endogenous EIN3 protein in seedlings grown on 1/2MS medium or 1/2MS medium with 10 ppm ethylene gas or 10 μM ACC treatment in darkness

for 3 days. Anti-EIN3 and anti-Actin antibodies were used for immunoblots. Actin was used as a loading control.

Gray boxes indicate WT, orange boxes indicate the *ein3 eil1* mutant, and green boxes indicate *ET-free* mutants, $n = 15$. Data are mean values ± SD. In **(B) and (D), ****P < 0.01, *0.01 < P < 0.05; P values were >0.05 between ein2–5 and ET-free mutants (Student's t-test).*** Scale bars, 1 mm.

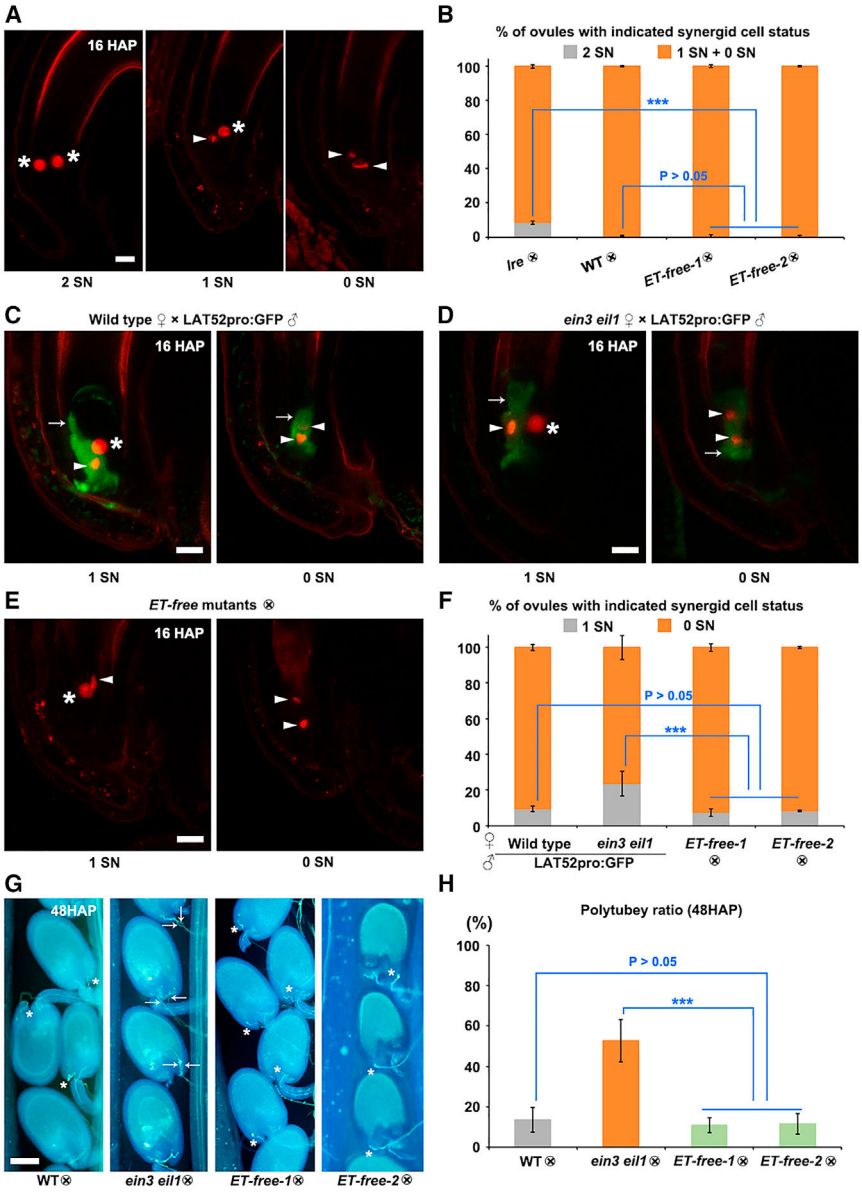

Figure 3. Degeneration of both synergid cells is not affected in *ET-free* mutants.

(A and B) Representative images and statistical analysis of synergid cell degeneration in self-crossed *lre*, WT, and *ET-free* mutants at 16 HAP; synergid cell degeneration was determined by examining the synergid nucleus marker *MYB98pro*:*H*$_2$*B-tdTOM* in *lre* (*n* = 351), WT (*n* = 307), and *ET-free* mutant (*ET-free-1*, *n* = 342; *ET-free-2*, *n* = 191) ovules. Asterisks indicate non-degenerated round synergid nuclei, and arrowheads point to degenerated synergid nuclei. Gray box in **(B)** represents the percentage of ovules with two synergid cell nuclei, while orange boxes show the percentage of ovules with one or no synergid cell nucleus.

(C–F) Representative images and statistical analysis of synergid cell degeneration in WT (*n* = 307) and *ein3 eil1* (*n* = 198) plants pollinated with *LAT52pro*:*GFP* pollen and in selfed *ET-free* mutants (*ET-free-1*, *n* = 342; *ET-free-2*, *n* = 191) at 16 HAP. Synergid cells were

labeled with *MYB98pro:H$_2$B-tdTOM*. Asterisks indicate non-degenerated round synergid nuclei, while arrowheads show degenerated and condensed synergid nuclei. Small arrows indicate fluorescence released from *LAT52pro:GFP*-labeled pollen tubes. Scale bars, 10 μm. Gray boxes in **(F)** indicate the percentage of ovules with one synergid nucleus, and orange boxes show the percentage of ovules with no synergid nucleus.

(G and H) Representative images of aniline blue staining of selfed WT (n = 12), *ein3 eil1* (n = 14), and *ET-free* mutants (*ET-free-1*, n = 18; *ET-free-2*, n = 10) at 48 HAP, and statistical analysis of polytubey. Asterisks indicate one pollen tube at the micropyle in WT and *ET-free* mutant ovules. Arrows point to polytubey at the micropyle in *ein3 ein1* ovules. Gray boxes indicate WT, orange boxes the *ein3 eil1* mutant, and green boxes the *ET-free* mutants. "×" in **(B)**, **(F)**, and **(H)** represents self-pollination. Analyses in **(B)** and **(F)** were performed using the same datasets. Data are mean values ± SD. ***$P < 0.01$, $P > 0.05$ between WT and *ET-free* mutants (Student's t-test). Scale bars, 100 μm.